J. Water Environ. Nanotechnol., 3(4): 301-310 Autumn 2018

ORIGINAL RESEARCH PAPER

Application of Green Novel NiO/ZSM-5 for Removal of Lead and Mercury ions from Aqueous Solution: Investigation of Adsorption Parameters

Mehdi Sedighi[1]* , Majid Mohammadi[2]

[1] *Department of Chemical Engineering, University of Qom, Qom, Iran*
[2] *Department of Energy Engineering, Faculty of Science, Qom University of Technology, Qom, Iran*

Received: 2018-06-26 Accepted: 2018-08-23 Published: 2018-10-15

ABSTRACT

Consistent with the US Environmental Protection Agency, heavy metals are classified as carcinogenic to humans. Their numerous agricultural, industrial, domestic, medical, and technical requirements have resulted in their widespread dissemination in the environment. This article examines a new green adsorbent for the removal of two hazardous heavy metals, lead, and mercury. The impact of contact time, pH, initial concentration, and temperature on the adsorption capacity of Pb^{2+} and Hg^{2+} were evaluated. Experimental data were analyzed by adsorption models. The equilibrium data were well adapted to the Langmuir adsorption model. The results show that the adsorption is homogeneous and localized in a monolayer. In addition, the maximum adsorption capacity was 277.78 mg/g for Pb^{2+} and 64.52 mg/g for Hg^{2+} from Langmuir isotherm. Thermodynamic data, including free energy (ΔG°), enthalpy (ΔH°), and entropy (ΔS°) variations were also considered. The important point is that the negative value of ΔG° signifies the spontaneity of the adsorption process of the heavy metals–NiO/ZSM-5 system.

Keywords: *Adsorption Capacity, Lead, Mercury, NiO/ZSM-5, Thermodynamic*

How to cite this article
Sedighi M, Mohammadi M. Application of Green Novel NiO/ZSM-5 for Removal of Lead and Mercury ions from Aqueous Solution: Investigation of Adsorption Parameters. J. Water Environ. Nanotechnol., 2018; 3(4): 301-310.
DOI: 10.22090/jwent.2018.04.003

INTRODUCTION

Water is very crucial for humans and other living beings. In the human body, more than 70% is fluid, such as blood, and all these fluids are mainly water. Bone marrow needs water to produce blood, and the blood transports oxygen from the lungs to the whole organism [1, 2]. In addition, water can maintain the temperature of the human body and provide natural materials with minerals. Water is not only important to the body; it also plays an important role in our daily activities, such as washing clothes and food, bathing for personal hygiene and solvent work for all reagents. Therefore, the water industry in this situation refers to a problem solver [3-5]. In the underdeveloped areas of the world, where there is no treatment facility, water-related diseases such as cholera, typhoid fever, and dysentery make a large number of people ill every year [6, 7]. Vitally, clean water is one of the most significant natural resources on the planet. Wastewater, which is essentially used water, is also an important resource, especially with recurring droughts and water shortages in many parts of the world. However, effluents contain many pollutants and can only be released after treatment. Wastewater treatment, therefore, has two important tasks: the restoration of water supply and the protection of the planet from toxins [8].

The heavy metal describes any metallic element

* Corresponding Author Email: *sedighi@qom.ac.ir*
sedighi.ac@gmail.com

with a relatively high density, which is harmful or toxic in small quantities. Heavy metals threaten as they appear to bioaccumulate. Bioaccumulation is an improvement for the compound in a biological organism during the period compared to the concentration of the chemical in nature. Substances that accumulate in living organisms when absorbed and collected faster than when degraded [2, 9, 10]. In human, exposure to lead may result in different biological effects, depending on the extent and duration of exposure. Different effects occur in a different dosage, with the growing fetus and the child becoming more sensitive than the adult. High amounts of contact can cause harmful biochemical impacts in mankind, leading to problems with hemoglobin synthesis, influence on the kidneys, joints and reproductive system, as well as a chronic problem on the nervous system [2, 11-13]. A number of reports indicate that a losing 2 IQ points could result in an increase in blood lead amounts of 10 to 20 µg/dL in young children [14-16].

In the United Kingdom, the typical daily exposure of lead in adults is expected to be 1.6 µg in the air, 20µg in drinking water and 28µg in food. Although the majority of people receive most of their lead intake, additional options can be essential in some populations, including water in areas with lead pipes and lead water, near air the source of emissions, land [17, 18].

Mercury is a poisonous material that has no identified performance in biochemistry or human physiology and does not naturally appear in living beings. Inorganic mercury poisoning is related to tremor, and /or minor psychological changes as well as miscarriages and birth defects [19-21]. Monomethylmercury and dimethylmercury are highly toxic and cause neurotoxic disorders [22, 23].

There are several methods of water purification, including adsorption technology, which is a wastewater treatment technique to remove many compounds from industrial wastewater. The adsorption is usually used for the removal or low concentration of non-degradable organic compounds in groundwater, in drinking water treatment, in process water or in tertiary treatment after, for example, biological water purification [24, 25].

Zeolites are among the most popular adsorbents in various industries. Zeolites are porous crystalline aluminosilicates comprising assemblages of SiO_4 and AlO_4 tetrahedra linked together by sharing oxygen atoms. In addition, the prospects for using nanomaterials with a diameter of less than 100 nm are currently extensively studied in many applications in various fields: physics, biology, cosmetics, chemistry, optical components, polymers pharmaceuticals, mechanics, toxicology and oil industry [26-28]. Nickel oxide (NiO), as a result of its high electrocatalytic properties, oxygen ion conductivity, biocompatibility, nontoxicity as well as high chemical stability is a potential candidate for the development of adsorption [29, 30]. Besides, the application of NiO for some adsorption process together with its beneficial is within the literature [29-33].

In this study, for the first time, green biobased template formed by decarboxylation of amino acids was utilized to prepare the crystalline microporous NiO/ZSM-5. The adsorption capacity was determined by isotherm models and thermodynamic parameters for the pollutant removal.

EXPERIMENTS

Material

Lead nitrate ($Pb(NO_3)_2$) and mercury standard solution were supplied by Merck, Germany. All other chemicals were sourced from Merck and Daejung (Busan, KOREA).

Synthesis of NiO/ZSM-5 material

Synthesis of ZSM-5. At first 1.4 g NaOH was dissolving in 8 mL bio-cadaverine (green template) in 65 mL of distilled water (making seeding gel). Then, 13.1 g silicic acid was added in portion with vigorous stirring. The resulting mixture was shaken for 1 hour at room temperature and aged at 100 °C for 10 hours. Then, the fixed amount of NaOH, $NaAlO_2$ and silicic acid were added to the mixture. The resulting mixture was stirred at room temperature for 1 hour. Then, seeding gel was included to the synthesis gel. The resulting mixture was treated in an autoclave at 180 °C for 40 hours. The prepared sample was filtered, dried and calcined.

Synthesis of NiO/ZSM-5. The NiO/ZSM-5 adsorbent was synthesized by incipient wetness impregnation. A solution of $Ni(NO_3)_2.6H_2O$ was slowly added to the ZSM-5 powder. The sample was then placed in the oven at 100°C for 12 hours. The resulting sample was then ground to powder and placed in the muffle furnace at 550 °C for 5 hours.

Adsorption experiment

To prepare a stock solution with various concentrations of Pb solution, we added 12.65 g of lead nitrate ($Pb(NO_3)_2$) (analytical reagent grade) to the nearest 0.1 mg. This material is then transferred to a 1 L volumetric flask, diluted with distilled water, and mixed thoroughly. The stock solution of mercury (II) with different concentrations was prepared by dissolving 0.25 g to 0.09 g of $HgCl_2$ in a 100 mL volumetric flask using double distilled water.

To demonstrate the adsorption properties of NiO/ZSM-5 in an aqueous solution of Pb(II) and Hg(II), a series of experiments were carried out to evaluate the effects of pH, contact time as well as initial concentration on pollutants. Batch tests were completed by closed types independently for each pollutant. The filter paper was applied for the filtration of the solution. The residual concentration of pollutants in the solution was regarded by atom fluorescence spectrophotometer (AFS, BRAIC) with an online reducing unit (AF-610A, China) with NaBH4 and HCl solution. The calibration, as well as performances of APS, is according to Ref. [34, 35].

The amount of adsorption capacity, q_e ($mg.g^{-1}$), was calculated using Eq. (1):

$$q_e = (\frac{C_0 - C_e}{m}) \times V \quad (1)$$

All parameters are determined in our previous work [3, 4, 36]. Moreover, setting pH was performed employing 0.1 M HCl and 0.1 M NaOH.

Characterization techniques

X-Ray diffraction (XRD, Bruker D8) is used for the investigation of crystalline materials using CuKa radiation (40 kV and 50 mA). FT-IR was performed using a Nicolet 370 spectrophotometer. This technique measures the absorption of infrared radiation by the sample material versus wavelength. The TEM image of the prepared sample was tested using the JEOL JEM-2010 200 kV Transmission Electron Microscope. The XRF study was accomplished using X-ray fluorescence (XRF, unisantis, XMF-104) to identify the percent of each component of the composite.

RESULT AND DISCUSSION

Characterization of the adsorbent

Fig. 1 shows the XRD patterns of the samples. The representative peaks happen at 2θ= 22.95, 23.8 and 24.35. The intensity of ZSM-5 signals decreased slightly after the introduction of nickel during synthesis which is coincided with different Ref. [37, 38]. After NiO loadings, no new crystalline phase was detected.

The TEM image of the NiO/ZSM-5 adsorption surface was provided in Fig. 2. As shown, the size of the NiO particles is between 20 and 35 nm, which agrees properly with the estimated results of the Scherrer's equation.

Table 1 represents the physicochemical properties for the synthesized sample. These results prove that the surface area and the actual content of

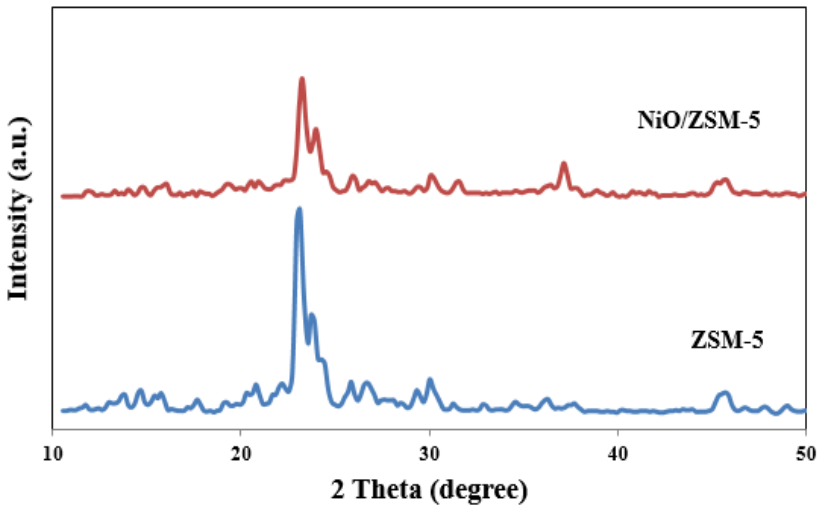

Fig. 1. XRD pattern of Nio/ZSM-5

NiO over the NiO/ZSM-5 sample are 348 m^2/g and 2.8 wt.%. From the XRF analysis, the Si/Al ratio of the modified sample is approximately similar to that of the gel solution and the Ni content is almost equivalent.

The FT-IR spectra of ZSM-5 and NiO/ZSM-5 are represented in Fig. 3. The IR spectrum indicates that the ZSM-5 has different vibrational bands, e.g. at 1234, 1075, 792, 546, 450 cm^{-1} which corresponded properly to Ref [39, 40]. All vibrational bands in the NiO/ZSM-5 framework were slightly shifted to a lower wavenumber than those of ZSM-5. These changes show that NiO particles can be incorporated into the ZSM-5 material [41].

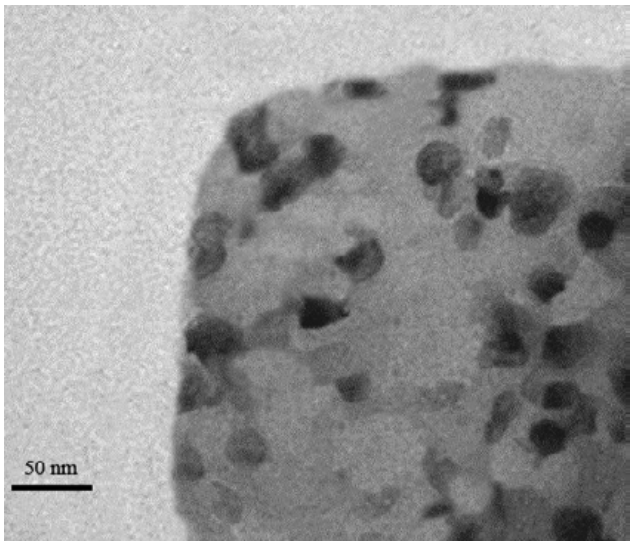

Fig. 2. TEM image of NiO/ZSM-5.

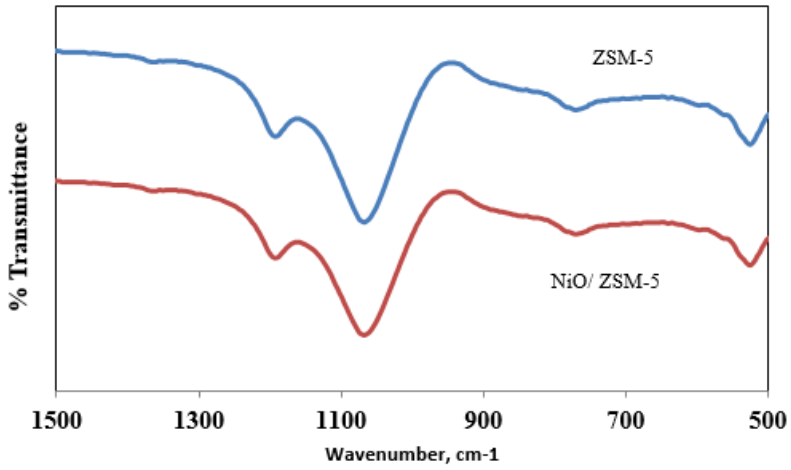

Fig. 3. FTIR pattern of adsorbent.

Table 1. Physico-chemical characteristics of crystalline samples

Sample	BET surface area [a] (m^2/g)	Total pore volume [a] (cm^3/g)	Si/Al [b]	Ni (wt.%) [b]
ZSM-5	405	0.183	38	–
NiO/ZSM-5	348	0.126	37	2.8

[a] From N_2 adsorption method (BET methods).
[b] By XRF analysis.

Effect of variables on the adsorption process

Fig. 4 indicates the effect of pH on the pollutant adsorption on NiO/ZSM-5. As shown, the adsorption capacity was low in the strongly acidic solution for both impurities. Improving the pH to 8 ensures better adsorption capacity. At low pH, the availability of H^+ would compete with Pb^{2+} and Hg^{2+} for adsorption sites on the surface of the adsorbent.

Fig. 5 presents the effect of contact time on adsorption capacity. As shown, the adsorption equilibrium was completed within 180 min for Hg^{2+} and 220 min for Pb^{2+}. These data prove that the equilibrium is attained in a short time.

The amount of adsorbed pollutants for various initial concentrations onto NiO/ZSM-5 was determined and shown in Fig. 6. To show the effect of adsorbent on water uptake, a specified amount of NiO/ZSM-5 sample was added to a 50 mL dilute aqueous solution (pH=8). The initial concentration of Hg (II) solution varies from 0.06 mg/L to 30 mg/L. Moreover, the initial concentration of Pb (II) solution ranged from 20 mg/L to 200 mg/L. The pollutant removal increases with an increase in the initial concentration of Hg^{2+} and Pb^{2+}. Main driving force for mass transfer is responsible for the adsorbent capacity increase.

Adsorption isotherms

The equilibrium data were examined by both Langmuir and Freundlich models, following two linear Eqs:

$$\frac{C_e}{q_e} = \frac{C_e}{q_m} + \frac{1}{K_L\, q_m} \tag{2}$$

$$\ln q_e = \ln K_F + \left(\frac{1}{n}\right) \ln C_e \tag{3}$$

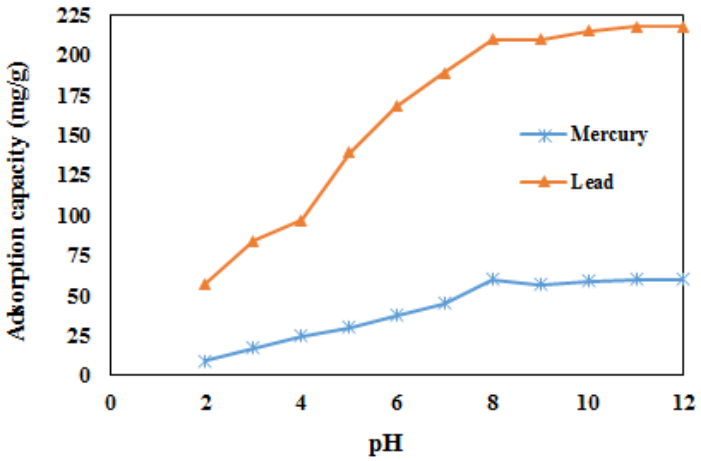

Fig. 4. Effect of solution pH on adsorption capacity (T=298 K, initial concentration for Pb(II) =100 mg/L and for Hg(II)= 20 mg/L).

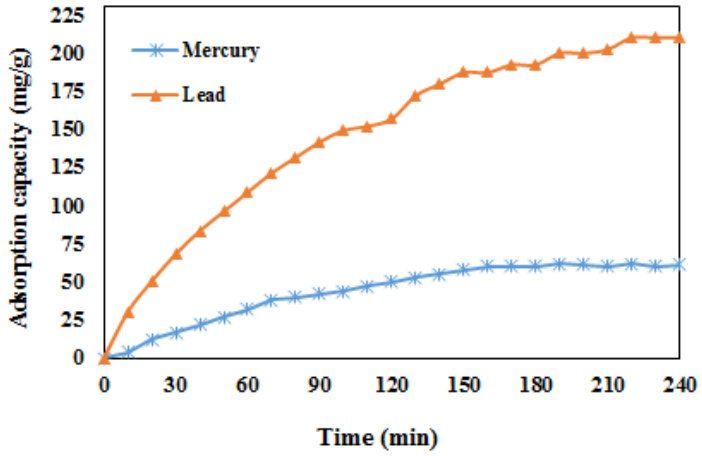

Fig. 5. Effect of contact time on adsorption capacity (pH=8, T=298 K, initial concentration for Pb(II) =100 mg/L and for Hg(II)= 20 mg/L).

All parameters are shown in our previous work [42-47]. The fitting results are shown in Figs. 7 and 8 and in Table 2. According to R^2, it is clear that the Langmuir model is more suitable for both pollutants than the Freundlich model. These findings show that the adsorption is homogeneous and localized in a monolayer. Besides, the larger the constant K_L, the higher is the adsorption energy, reflected by a quick increase in adsorption at low adsorbate concentrations [44]. Furthermore, *1/n* values is in the range $0.1 < 1/n < 1$, what signifies that adsorption was favorable [48]. The maximum monolayer adsorption capacity (q_m) was detected to be 64.52 mg/g for mercury and 277.78 mg/g for the lead.

Table 3 and 4 show comparison of mercury and lead adsorption capacity of this study and other adsorbents.

Adsorption Thermodynamics

The impact of temperature on the adsorption capacity of NiO/ZSM-5 nanocomposite at pH=8 is presented in Fig. 9. As observed in Fig. 9a, the adsorption capacity raises from 60 to 106 for Hg^{2+} and 210 to 256 for Pb^{2+} with rising temperature. This reveals the endothermic nature of the adsorption. Thermodynamic parameters, ΔH°, ΔG°, and ΔS° can be approximated using equilibrium constants

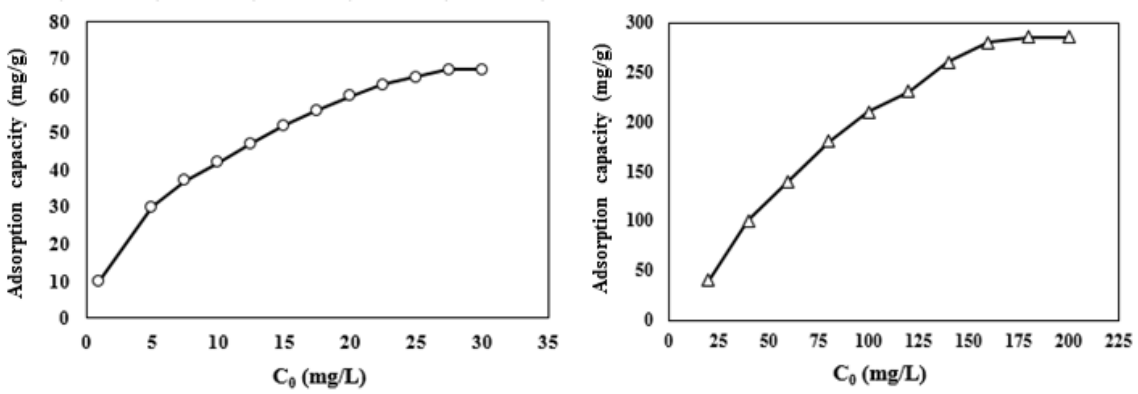

Fig. 6. Effect of initial concentration of Hg^{2+} (left) and Pb^{2+} (right) adsorption onto NiO/ZSM-5 (pH=8, T=298 K, contact time for Pb (II)=220 min and for Hg (II)=180 min).

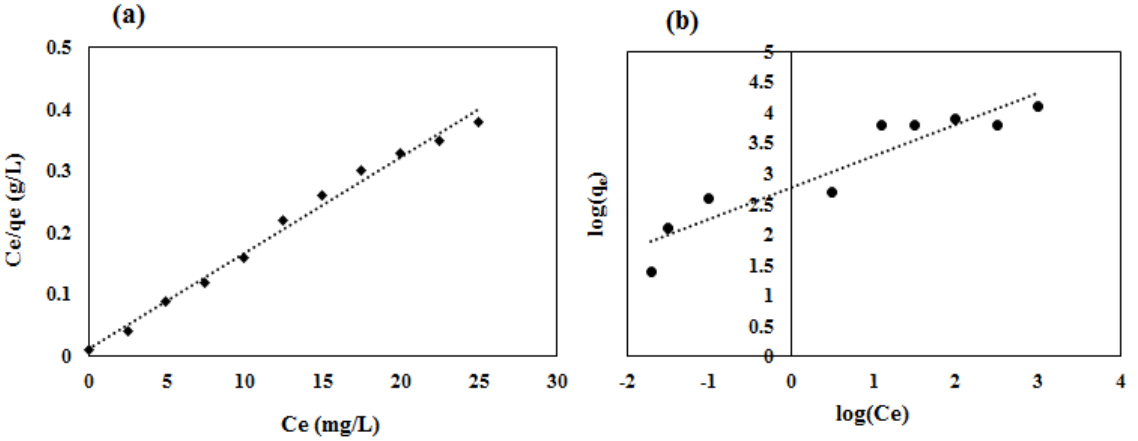

Fig. 7. (a) Langmuir isotherms for Hg^{2+} adsorption onto NiO/ZSM-5. (b) Freundlich isotherms for Hg^{2+} adsorption onto NiO/ZSM-5.

Table 2. Adsorption isotherm constants

	Langmuir			Freundlich		
	q_m (mg. g^{-1})	K_L(L. mg^{-1})	R^2	Log (K_F)	*1/n*	R^2
Mercury	64.52	1.35	0.98	1.39	0.71	0.88
Lead	277.78	0.783	0.99	1.65	0.68	0.81

Table 3. Comparison of the mercury ion adsorption capacities of the various adsorbent.

Adsorbents	Adsorption capacity (mg/g)	Temperature (˚C)	Ref.
SDS–MC	8.9	25	[49]
CTAB–MC	8.1	25	[49]
MC	7.4	25	[49]
Nitrogen-doped magnetic CNTs	2.59 mmol/g	25	[50]
SH-Beta/MCM-41	8.2	25	[51]
MnO_2-coated carbon nanotubes	14.28	50	[52]
Phenolic hydroxyl functional group P-MWCNT	28.22	25	[53]
MWCNTs	7.092	25	[54]
MnO_2/CNT	58.8	25	[52]
NiO/ZSM-5	64.52	25	this study

Table 4. Comparison of the lead ion adsorption capacities of the various adsorbent.

Adsorbents	Adsorption capacity (mg/g)	Temperature (˚C)	Ref.
Activated carbon	20.9	25	[55]
Biochar	93.6	25	[55]
MWCNTs/ Fe_3O_4	13.04	25	[56]
Manganese oxide coated crushed brick	6.42	20	[57]
GO/Fe_3O_4-g-G3.0	181.4	25	[58]
Fe_3O_4@SiO_2-EDTA	114.94	30	[59]
Manganese oxide-coated carbon nanotubes	78.74	25	[60]
Manganese oxide-coated zeolite	74.9	30	[61]
Nanohydroxyapatite–alginate composite	270.3	25	[62]
NiO/ZSM-5	277.78	25	this study

Table 5. Adsorption thermodynamic data.

Metal ion	T (°C)	ΔG° (kJ mol^{-1})	ΔH° (kJ mol^{-1})	ΔS° (J K^{-1} mol^{-1})
Hg^{2+}	298	-0.495	22.26	88.97
	308	-0.614		
	318	-0.793		
	328	-0.899		
Pb^{2+}	298	-4.33	3.66	13.93
	308	-5.12		
	318	-5.82		
	328	-7.09		

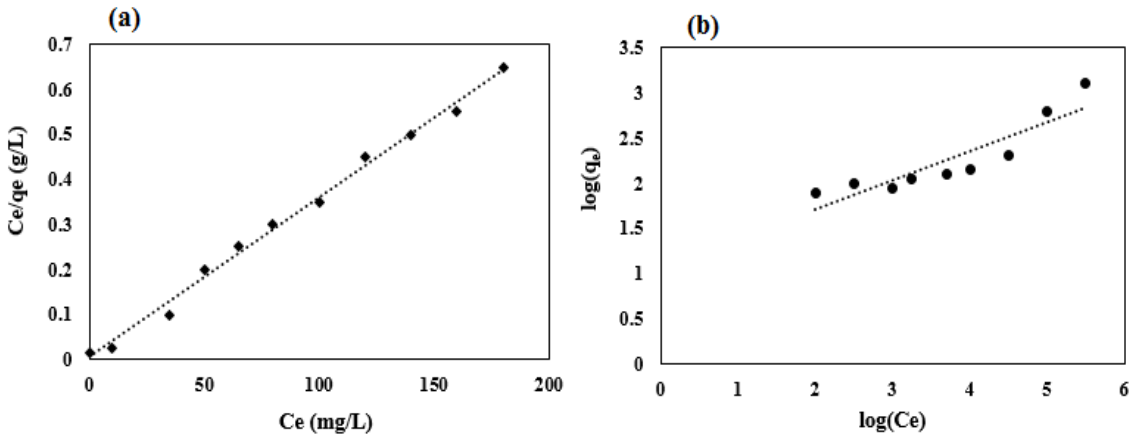

Fig. 8. (a) Langmuir isotherms for Pb^{2+} adsorption onto NiO/ZSM-5. (b) Freundlich isotherms for Pb^{2+} adsorption onto NiO/ZSM-5.

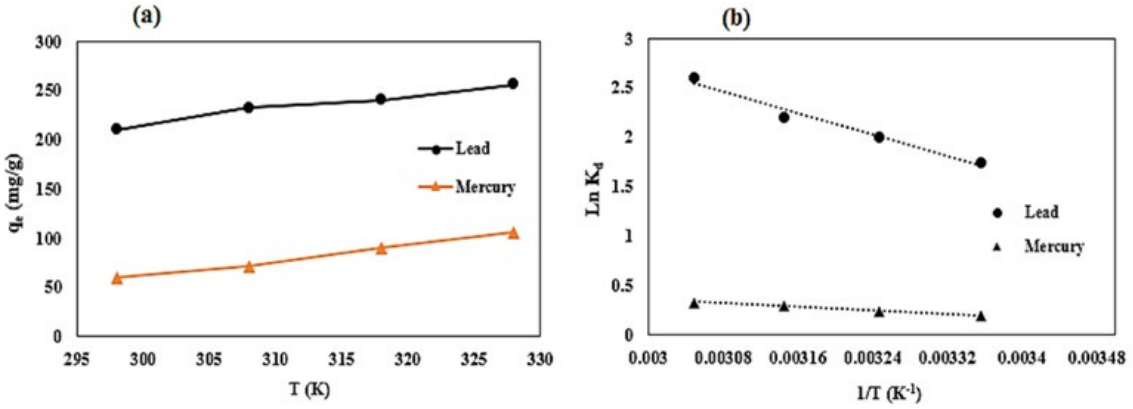

Fig. 9. Effect of temperature on (a) adsorption capacity and (b) Van't Hoff plot

that correlate with temperature:

$$K_d = \frac{q_e}{C_e} \quad (4)$$

$$\Delta G^\circ = -RT \ln K_d \quad (5)$$

$$\ln K_d = \frac{\Delta S^\circ}{R} - \frac{\Delta H^\circ}{RT} \quad (6)$$

The ΔG° values at different temperatures were calculated according to equation (5). ΔH° and ΔS° are calculated from the slope and intercept of equation (6) of ln K_d vs T^{-1} (Fig. 9b) and the calculated values are given in Table 5. The results show that the adsorption process of all examined metal ions was effective and spontaneous in nature as proved by the negative values of ΔG° and positive ΔH°. Additionally, the positive ΔS° showed that the degrees of freedom improved at the solid-liquid interface during the adsorption procedure.

CONCLUSION

To improve the removal of mercury and lead in water, a green and novel NiO/ZSM-5 adsorbent was synthesized. The XRD and FTIR analysis confirmed that no new crystalline phase was detected after the NiO charges, which means that the skeletal structure of the molecular sieve does not change. Due to the experimental results, the removal of pollutant was low in the strongly acidic solution. Increasing pH to 8 leads to an improvement of the adsorption capacity. In addition, pollutant removal increased with the initial concentration of Hg^{2+} and Pb^{2+}. The isotherm models showed that the Langmuir model is better suited for both pollutants than the Freundlich. These results show that the adsorption is homogeneous and localized in a monolayer. In addition, the thermodynamic analysis revealed that the process is beneficial, spontaneous and endothermic. The entire outcomes recommend that the existing green and novel nanocomposite verified to be a potential adsorbent for the removal of toxic heavy metals from the aquatic environment.

CONFLICT OF INTEREST

The authors declare that there are no conflicts of interest regarding the publication of this manuscript.

REFERENCES

1. Alimohammadi V, Sedighi M, Jabbari E. Optimization of sulfate removal from wastewater using magnetic multi-walled carbon nanotubes by response surface methodology. Water Science and Technology. 2017;76(10):2593-602.
2. Hua M, Zhang S, Pan B, Zhang W, Lv L, Zhang Q. Heavy metal removal from water/wastewater by nanosized metal oxides: A review. Journal of Hazardous Materials. 2012;211-212:317-31.
3. Alimohammadi V, Sedighi M, Jabbari E. Experimental study on efficient removal of total iron from wastewater using magnetic-modified multi-walled carbon nanotubes. Ecological Engineering. 2017;102:90-7.
4. Alimohammadi V, Sedighi M, Jabbari E. Response surface modeling and optimization of nitrate removal from aqueous solutions using magnetic multi-walled carbon nanotubes. Journal of Environmental Chemical Engineering. 2016;4(4):4525-35.
5. Fu F, Wang Q. Removal of heavy metal ions from wastewaters: A review. Journal of Environmental Management. 2011;92(3):407-18.
6. Alimohammadi V, Sedighi M. Reduction of TDS in Water by Using Magnetic Multiwalled Carbon Nanotubes and Optimizing with Response Surface Methodology. Journal of Environmental Engineering. 2018;144(3):04017114.

7. Nomanbhay SM, Palanisamy K. Removal of heavy metal from industrial wastewater using chitosan coated oil palm shell charcoal. Electronic Journal of Biotechnology. 2005;8(1).
8. Alimohammadi V, Sedighi M, Jabbari E, Nasrollahzadeh M. Phosphate removal from aqueous solutions using magnetic multi-walled carbon nanotube; optimization by response surface methodology. DESALINATION AND WATER TREATMENT. 2017;82:271-81.
9. Meena AK, Mishra GK, Rai PK, Rajagopal C, Nagar PN. Removal of heavy metal ions from aqueous solutions using carbon aerogel as an adsorbent. Journal of Hazardous Materials. 2005;122(1-2):161-70.
10. Amuda OS, Giwa AA, Bello IA. Removal of heavy metal from industrial wastewater using modified activated coconut shell carbon. Biochemical Engineering Journal. 2007;36(2):174-81.
11. Meena AK, Kadirvelu K, Mishra GK, Rajagopal C, Nagar PN. Adsorptive removal of heavy metals from aqueous solution by treated sawdust (Acacia arabica). Journal of Hazardous Materials. 2008;150(3):604-11.
12. Ghaedi M, Shokrollahi A, Kianfar AH, Mirsadeghi AS, Pourfarokhi A, Soylak M. The determination of some heavy metals in food samples by flame atomic absorption spectrometry after their separation-preconcentration on bis salicyl aldehyde, 1,3 propan diimine (BSPDI) loaded on activated carbon. Journal of Hazardous Materials. 2008;154(1-3):128-34.
13. Pagnanelli F, Mainelli S, Vegliò F, Toro L. Heavy metal removal by olive pomace: biosorbent characterisation and equilibrium modelling. Chemical Engineering Science. 2003;58(20):4709-17.
14. Gupta VK, Agarwal S, Saleh TA. Synthesis and characterization of alumina-coated carbon nanotubes and their application for lead removal. Journal of Hazardous Materials. 2011;185(1):17-23.
15. Saleh TA, Gupta VK. Column with CNT/magnesium oxide composite for lead(II) removal from water. Environmental Science and Pollution Research. 2011;19(4):1224-8.
16. Günay A, Arslankaya E, Tosun İ. Lead removal from aqueous solution by natural and pretreated clinoptilolite: Adsorption equilibrium and kinetics. Journal of Hazardous Materials. 2007;146(1-2):362-71.
17. Axtell, N.R., S.P. Sternberg, and K. Claussen, *Lead and nickel removal using Microspora and Lemna minor.* Bioresource technology, 2003. **89**(1): p. 41-48.
18. Abdel-Halim SH, Shehata AMA, El-Shahat MF. Removal of lead ions from industrial waste water by different types of natural materials. Water Research. 2003;37(7):1678-83.
19. Zhang F-S, Nriagu JO, Itoh H. Mercury removal from water using activated carbons derived from organic sewage sludge. Water Research. 2005;39(2-3):389-95.
20. Chiarle, S., M. Ratto, and M. Rovatti, *Mercury removal from water by ion exchange resins adsorption.* Water Research, 2000. **34**(11): p. 2971-2978.
21. Parham H, Zargar B, Shiralipour R. Fast and efficient removal of mercury from water samples using magnetic iron oxide nanoparticles modified with 2-mercaptobenzothiazole. Journal of Hazardous Materials. 2012;205-206:94-100.
22. Pérez-Quintanilla D, Hierro Id, Fajardo M, Sierra I. 2-Mercaptothiazoline modified mesoporous silica for mercury removal from aqueous media. Journal of Hazardous Materials. 2006;134(1-3):245-56.
23. Skubal LR, Meshkov NK. Reduction and removal of mercury from water using arginine-modified TiO2. Journal of Photochemistry and Photobiology A: Chemistry. 2002;148(1-3):211-4.
24. Ali I, Gupta VK. Advances in water treatment by adsorption technology. Nature Protocols. 2007;1(6):2661-7.
25. Faust, S.D. and O.M. Aly, *Adsorption processes for water treatment*. 2013: Elsevier.
26. Baerlocher, C., L.B. McCusker, and D.H. Olson, *Atlas of zeolite framework types*. 2007: Elsevier.
27. Mohammadi M, Dadvar M, Dabir B. TiO 2 /SiO 2 nanofluids as novel inhibitors for the stability of asphaltene particles in crude oil: Mechanistic understanding, screening, modeling, and optimization. Journal of Molecular Liquids. 2017;238:326-40.
28. Mohammadi M, Dadvar M, Dabir B. Application of response surface methodology for optimization of the stability of asphaltene particles in crude oil by TiO2/SiO2 nanofluids under static and dynamic conditions. Journal of Dispersion Science and Technology. 2017;39(3):431-42.
29. Behnajady MA, Bimeghdar S. Synthesis of mesoporous NiO nanoparticles and their application in the adsorption of Cr(VI). Chemical Engineering Journal. 2014;239:105-13.
30. Abu Tarboush BJ, Husein MM. Adsorption of asphaltenes from heavy oil onto in situ prepared NiO nanoparticles. Journal of Colloid and Interface Science. 2012;378(1):64-9.
31. Sheela T, Nayaka YA. Kinetics and thermodynamics of cadmium and lead ions adsorption on NiO nanoparticles. Chemical Engineering Journal. 2012;191:123-31.
32. Cheng B, Le Y, Cai W, Yu J. Synthesis of hierarchical Ni(OH)2 and NiO nanosheets and their adsorption kinetics and isotherms to Congo red in water. Journal of Hazardous Materials. 2011;185(2-3):889-97.
33. Motahari F, Mozdianfard MR, Salavati-Niasari M. Synthesis and adsorption studies of NiO nanoparticles in the presence of H2acacen ligand, for removing Rhodamine B in wastewater treatment. Process Safety and Environmental Protection. 2015;93:282-92.
34. Yu, F. and T. Yu, *HG-AFS determination of ultratrace Pb and Hg in underground water after sulfhydryl cotton preconcentration.* Guang pu xue yu guang pu fen xi= Guang pu, 2000. **20**(6): p. 898-900.
35. Sánchez-Rodas D, Corns WT, Chen B, Stockwell PB. Atomic Fluorescence Spectrometry: a suitable detection technique in speciation studies for arsenic, selenium, antimony and mercury. Journal of Analytical Atomic Spectrometry. 2010;25(7):933.
36. Sedighi M, Mohammadi M, Sedighi M, Ghasemi M. Biobased Cadaverine as a Green Template in the Synthesis of NiO/ZSM-5 Nanocomposites for Removal of Petroleum Asphaltenes: Financial Analysis, Isotherms, and Kinetics Study. Energy & Fuels. 2018;32(7):7412-22.
37. Batista, M., et al., *Iron species present in Fe/ZSM-5 catalysts–influence of the preparation method.* Hyperfine interactions, 2001. **134**(1): p. 161-166.
38. Rauscher M. Preparation of a highly active Fe-ZSM-5 catalyst through solid-state ion exchange for the catalytic decomposition of N2O. Applied Catalysis A: General. 1999;184(2):249-56.
39. Cheng Y, Wang L-J, Li J-S, Yang Y-C, Sun X-Y. Preparation and characterization of nanosized ZSM-5 zeolites in the absence of organic template. Materials Letters. 2005;59(27):3427-30.
40. Ismail AA, Mohamed RM, Fouad OA, Ibrahim IA. Synthesis of nanosized ZSM-5 using different alumina sources.

Crystal Research and Technology. 2006;41(2):145-9.
41. O'Malley AJ, Parker SF, Chutia A, Farrow MR, Silverwood IP, García-Sakai V, et al. Room temperature methoxylation in zeolites: insight into a key step of the methanol-to-hydrocarbons process. Chemical Communications. 2016;52(14):2897-900.
42. Mohammadi M, Ameri Shahrabi MJ, Sedighi M. Comparative study of linearized and non-linearized modified Langmuir isotherm models on adsorption of asphaltene onto mineral surfaces. Surface Engineering and Applied Electrochemistry. 2012;48(3):234-43.
43. Mohammadi M, Khamehchi E, Sedighi M. The Prediction of Asphaltene Adsorption Isotherm Constants on Mineral Surfaces. Petroleum Science and Technology. 2014;32(7):870-7.
44. Mohammadi, M., S.A. Mousavi-Dehghani, and M.J.A. Shahrabi. *Experimental investigation of asphaltene adsorption on different mineral surfaces and effect of various parameters on the adsorption rate: Study of adsorption with UV spectroscopy*. 2012. Abstracts of Papers of the American Chemical Society; American Chemical Soc.: Washington DC, 2012.
45. Mohammadi M, Sedighi M. Modification of Langmuir isotherm for the adsorption of asphaltene or resin onto calcite mineral surface: Comparison of linear and non-linear methods. Protection of Metals and Physical Chemistry of Surfaces. 2013;49(4):460-70.
46. Mohammadi M, Sedighi M, Hashemi Kiasari H, Hosseini SM. Genetic Algorithm Development for Prediction of Modified Langmuir Isotherm Parameters of Asphaltene Adsorption onto Metal Surfaces: Using Novel Quartz Crystal Nanobalance. Journal of Dispersion Science and Technology. 2014;36(3):384-92.
47. Mousavi-Dehghani, S.A. and M. Mohammadi, *A study of asphaltene adsorption manner on reservoir rock surfaces with application of langmuir isotherm modification*. Petroleum research, 2014. **23**(76): p. 154-167.
48. Sedighi M, Mohammadi M, Sedighi M. Green SAPO-5 supported NiO nanoparticles as a novel adsorbent for removal of petroleum asphaltenes: Financial assessment. Journal of Petroleum Science and Engineering. 2018;171:1433-42.
49. Anbia M, Amirmahmoodi S. Removal of Hg (II) and Mn (II) from aqueous solution using nanoporous carbon impregnated with surfactants. Arabian Journal of Chemistry. 2016;9:S319-S25.
50. Shin K-Y, Hong J-Y, Jang J. Heavy metal ion adsorption behavior in nitrogen-doped magnetic carbon nanoparticles: Isotherms and kinetic study. Journal of Hazardous Materials. 2011;190(1-3):36-44.
51. Fardmousavi O, Faghihian H. Thiol-functionalized hierarchical zeolite nanocomposite for adsorption of Hg2+ from aqueous solutions. Comptes Rendus Chimie. 2014;17(12):1203-11.
52. Moghaddam HK, Pakizeh M. Experimental study on mercury ions removal from aqueous solution by MnO 2 / CNTs nanocomposite adsorbent. Journal of Industrial and Engineering Chemistry. 2015;21:221-9.
53. Chen PH, Hsu C-F, Tsai DD-W, Lu Y-M, Huang W-J. Adsorption of mercury from water by modified multi-walled carbon nanotubes: adsorption behaviour and interference resistance by coexisting anions. Environmental Technology. 2014;35(15):1935-44.
54. Gupta A, Vidyarthi SR, Sankararamakrishnan N. Enhanced sorption of mercury from compact fluorescent bulbs and contaminated water streams using functionalized multiwalled carbon nanotubes. Journal of Hazardous Materials. 2014;274:132-44.
55. Cao X, Ma L, Gao B, Harris W. Dairy-Manure Derived Biochar Effectively Sorbs Lead and Atrazine. Environmental Science & Technology. 2009;43(9):3285-91.
56. Ji L, Zhou L, Bai X, Shao Y, Zhao G, Qu Y, et al. Facile synthesis of multiwall carbon nanotubes/iron oxides for removal of tetrabromobisphenol A and Pb(ii). Journal of Materials Chemistry. 2012;22(31):15853.
57. Boujelben N, Bouzid J, Elouear Z. Removal of Lead(II) Ions from Aqueous Solutions Using Manganese Oxide-Coated Adsorbents: Characterization and Kinetic Study. Adsorption Science & Technology. 2009;27(2):177-91.
58. Ma Y-X, Kou Y-L, Xing D, Jin P-S, Shao W-J, Li X, et al. Synthesis of magnetic graphene oxide grafted polymaleicamide dendrimer nanohybrids for adsorption of Pb(II) in aqueous solution. Journal of Hazardous Materials. 2017;340:407-16.
59. Liu Y, Fu R, Sun Y, Zhou X, Baig SA, Xu X. Multifunctional nanocomposites Fe 3 O 4 @SiO 2 -EDTA for Pb(II) and Cu(II) removal from aqueous solutions. Applied Surface Science. 2016;369:267-76.
60. Wang S, Gong W, Liu X, Yao Y, Gao B, Yue Q. Removal of lead(II) from aqueous solution by adsorption onto manganese oxide-coated carbon nanotubes. Separation and Purification Technology. 2007;58(1):17-23.
61. Zou W, Han R, Chen Z, Shi J, Liu. Characterization and Properties of Manganese Oxide Coated Zeolite as Adsorbent for Removal of Copper(II) and Lead(II) Ions from Solution. Journal of Chemical & Engineering Data. 2006;51(2):534-41.
62. Googerdchian F, Moheb A, Emadi R. Lead sorption properties of nanohydroxyapatite–alginate composite adsorbents. Chemical Engineering Journal. 2012;200-202:471-9.